Organic & Biomolecular Chemistry

Cite this: *Org. Biomol. Chem.*, 2012, **10**, 2385

www.rsc.org/obc

COMMUNICATION

Intramolecular proton transfer impact on antibacterial properties of ansamycin antibiotic rifampicin and its new amino analogues†

Krystian Pyta,[a] Piotr Przybylski,*[a] Barbara Wicher,[a] Maria Gdaniec[a] and Joanna Stefańska[b]

Received 2nd January 2012, Accepted 27th January 2012
DOI: 10.1039/c2ob00008c

Intramolecular proton transfer in rifampicin (1) and its analogues 2–9 with the formation of zwitterions has been indicated by multinuclear NMR and crystallographic studies. Biological tests of 1–9 in combination with the analysis of ligand–protein interactions have revealed the relationship between the protonation site and extremely high antibacterial activity.

Rifampicin (Scheme 1) belongs to a wide group of antibiotics called rifamycins that have been at the top of clinically used pharmaceuticals against tuberculosis over the last 35 years.[1,2] Antibacterially active rifamycins inhibit DNA-dependent RNA polymerase (RNAP) by binding to the RNAP β subunit *via* hydrogen bonds and hydrophobic interactions at a site about 12 Å away from Mg^{2+} ions.[3] The presence of a naphthalene ring with quinone or hydroquinone oxygen atoms at C-1 and C-8 and two hydroxyl groups at C-21 and C-23 of the ansa chain, which have to be in a particular spatial arrangement, is essential for antibacterial activity.[4] The rifampicin molecule is relatively rigid with conformational flexibility largely restricted by a system of intramolecular hydrogen bonds. Moreover, owing to the presence of both acidic (phenols) and basic (amine, hydrazone) groups within the molecule, an intramolecular proton transfer can occur resulting in neutral (phenolic) and zwitterionic (phenolate) forms of this antibiotic (Scheme 2). This aspect of the rifampicin structure, postulated already in 1975 by Ferrari and Gallo,[5] has been little studied and not taken into account in some later spectroscopic reports.[6,7] Also the crystal structures of rifampicin solvates, due to their low accuracy, were not reliable with respect of neutral *versus* zwitterionic form of rifampicin present in the crystal.[8,9] Thus, it is not surprising that only the neutral form of rifampicin, or its analogues, has been considered when constructing the ligand–protein interaction model on the basis of the crystal structures of rifampicin–protein complexes.[3] All above considerations and earlier findings have prompted us to explain the problem of localisation of protons from phenolic groups within **1** and its derivatives and encouraged us to clarify the biological role of the substituent at C-3 atom.

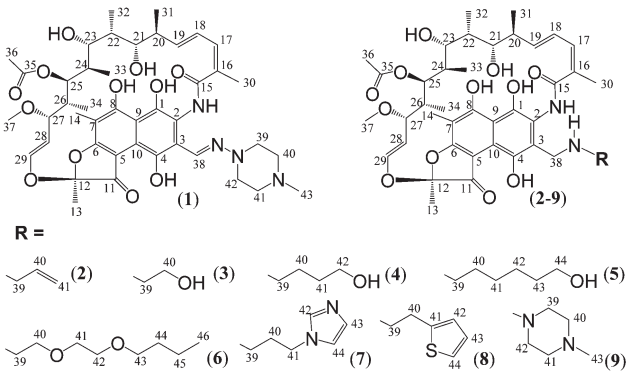

Scheme 1 Rifampicin (**1**) and its amino analogues **2–9**.

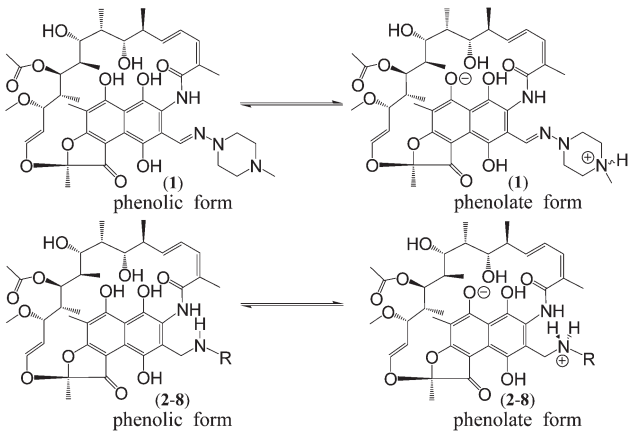

Scheme 2 Possible uncharged (phenolic) and zwitterionic (phenolate) forms of **1** and **2–8**.

The crystal structures of solvated forms of **1**, **1**-CH_3CCl_3 and **1**-CH_3OH–H_2O, clearly showed that from aprotic CH_3CCl_3 solvent, **1** crystallized in the phenolic form with a proton attached to O(8) (Fig. 1a) whereas when crystallized from

[a]*Faculty of Chemistry, A. Mickiewicz University, Grunwaldzka 6, 60-780 Poznan, Poland. E-mail: piotrp@amu.edu.pl; Fax: +48 618291505; Tel: +48 61 8291252*
[b]*Medical University of Warsaw, Department of Pharmaceutical Microbiology, Oczki 3, 02-007 Warsaw, Poland*

†Electronic supplementary information (ESI) available: Experimental details, FT-IR, 1D and 2D NMR data for **1–9**, crystallographic data for **1**-CH_3CCl_3, **1**-CH_3OH–H_2O and **2**-CH_3OH–CH_2Cl_2, extended biological data for compounds **1–9**. CCDC 859792–859794. For crystallographic data in CIF or other electronic format see DOI: 10.1039/c2ob00008c

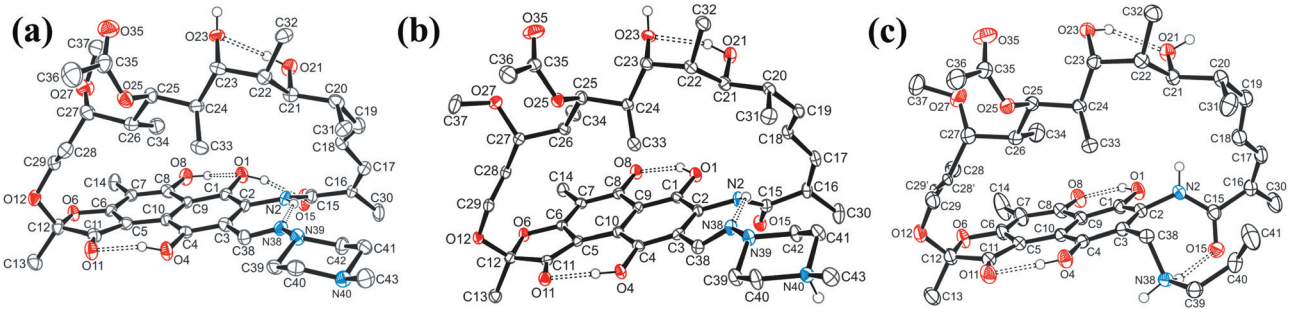

Fig. 1 Crystal structures of: (a) **1**-CH_3CCl_3, (b) **1**-CH_3OH–H_2O, (c) **2**-CH_3OH–CH_2Cl_2, indicating different localisation of the acidic proton from O(8)–H phenol group within molecules in solid.

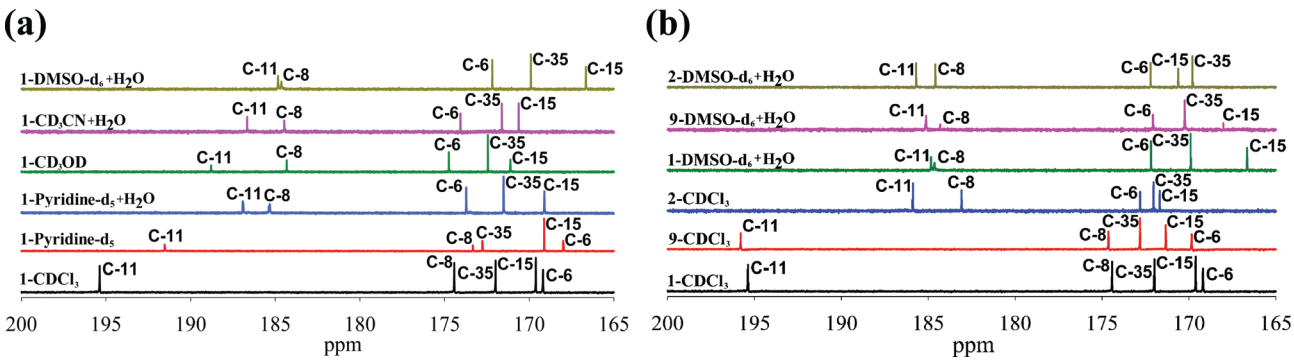

Fig. 2 ^{13}C NMR spectra of: (a) **1** and (b) **2** and **9**, recorded in protic and aprotic solvents with or without addition of H_2O.

methanol the phenolate form was obtained with protonated N(40) atom of the piperazine group (Fig. 1b). The proton transfer has a strong impact on a system of intramolecular interactions within **1**, as the collective system of four intramolecular hydrogen bonds can be formed solely in the phenolic form (Table S1†). In turn, in the phenolate form, breaking of the intramolecular O(1)–H···O(15) bond involving the amide carbonyl group increases the conformational freedom about the bond of the amide group with the naphthalene fragment, strongly influencing the conformation of the ansa chain and its orientation relative to the aromatic fragment. Thus, conformations of **1** in the phenolic and phenolate forms should substantially differ, affecting the docking process of this molecule at its RNAP binding site. The crystal structure of the rifampicin derivative **2** (**2**-CH_3OH–CH_2Cl_2, Fig. 1c) also reveals the phenolate form with a proton attached to the N(38) atom of the amine group. This group is involved in a strong intramolecular hydrogen bond with the carbonyl oxygen atom of the amide fragment that is nearly perpendicularly oriented with respect to the aromatic system (Fig. 1c). In effect, the rigidity of the ansa chain in **2** is increased relative to that in **1**.

To study the proton transfer process in **1** and **2**–**9** the multinuclear 1D and 2D NMR experiments were performed in solvents of different dielectric constants with and without addition of water (Fig. 2 and Fig. 1S–11S, Tables 3S and 4S†). Analysis of the 165–200 ppm range for **1** (Fig. 2a) revealed that the position of C-6, C-8 and C-11 signals in the spectra is strongly dependent on the type of solvent used. In the aprotic solvents such as $CDCl_3$, pyridine-d_5 and CD_3CN C-11 ($\delta_{in\ CDCl_3}$ = 195.3, $\delta_{in\ py\text{-}d_5}$ = 191.6 and $\delta_{in\ CD_3CN}$ = 190.7 ppm) and C-8 ($\delta_{in\ CDCl_3}$ = 174.5, $\delta_{in\ py\text{-}d_5}$ = 173.1, $\delta_{in\ CD_3CN}$ = 172.8 ppm) resonances indicate the localisation of the proton at the O(8) oxygen and the presence of the phenolic form of **1**. This conclusion is also supported by the ^1H NMR spectra and ^1H–^{13}C HMBC correlations (Fig. 8S†) which reveal $\delta_{O(8)H}$ resonances at 11.98 ($CDCl_3$), 12.58 (py-d_5) and 12.30 (CD_3CN) ppm and (H_8)spin–(C)spin couplings with neighbouring C-7, C-8 and C-9 carbons, respectively. Furthermore, the $\delta_{O(8)H}$ value clearly demonstrates the engagement of O(8)H group in the intramolecular hydrogen bond with O(1) oxygen in all aprotic solvents, similar to the crystal (Fig. 1a). However, in protic systems such as CD_3OD and DMSO-d_6 + H_2O, the C-8 resonances of **1** are shifted significantly toward higher ppm values up to about 185 ppm (Fig. 2a). This shift is a consequence of a proton transfer from O(8)H group and the appearance of negative charge at O(8) delocalised as a result of a strong resonance with the ketone group in *para* position. Additional evidence of this proton transfer is provided by the fact that the C-11 resonance of ketone moiety is strongly shielded if compared with that of $\delta_{C\text{-}11}$ region characteristic of **1** phenolic form in $CDCl_3$, py-d_5 and CD_3CN. Now the question of where the proton transferred from O(8)H phenolic group of **1** in protic solvents is localised arises. As follows from ^1H–^{15}N HSQC and HMBC spectra of **1** in DMSO-d_6 + H_2O (Fig. 1S and 2S†) the nitrogen atom signals at: −30, −252, −255 and −340 ppm are assigned to N(38), N(2) –H, N(39) and the positively charged N^+(40) atom, respectively. Thus, in protic solvents, the proton of O(8)H is transferred to nitrogen N(40) and **1** exists in the phenolate form. As shown in Fig. 2a the addition of H_2O to **1** dissolved in aprotic solvents resulted in deshielding of $\delta_{C\text{-}8}$ resonances, which is evidence for the proton transfer within

Table 1 Antibacterial activity MIC(μg mL^{-1}) of **1**, CIP and **2–9**

Bacteria strain	**1**	**2–8**	**9**	CIP
S. aureus NCTC 4163	0.008	0.5–2	0.008	0.5
S. aureus ATCC 25923	0.016	1–2	0.016	0.5
S. aureus ATCC 6538	0.008	0.5–2	0.008	0.5
S. aureus ATCC 29213	0.008	0.5–2	0.008	0.5
S. epidermidis ATCC 12228	0.008	0.125–0.25	0.008	0.5

1 and formation of the zwitterionic form and the key role of H_2O molecules in this process. The uncharged and zwitterionic forms of **1** (Scheme 2) in protic and aprotic solvents are reflected in the respective crystal structures (Fig. 1a and b). A comparison of the signals in the range 165–200 ppm between the ^{13}C NMR spectra of **1** (Fig. 2a) and **9** (Fig. 2b) indicated that **9** exists in the phenolate form in protic solvents and in the phenolic one in aprotic solvents, analogously to **1**. In contrast to **1** and **9**, the ^{1}H, ^{13}C and ^{15}N NMR data of derivatives **2–8** (Fig. 2b, 3S and 4S and Tables 3S and 4S†) revealed in their structures the exclusive presence of the phenolate form (Scheme 2), irrespective of whether they are dissolved in protic or aprotic systems. The proton transferred from the O(8)H group in structures **2–8** in solution is localised, however at the N(38) atom of the highest basicity as indicated by the ^{1}H–^{15}N HSQC correlation (Fig. 4S†). Thus, the presence of the zwitterionic form and the localisation of the transferred proton both in the crystal of **2** (Fig. 1c) and in structures **2–8** in solution are consistent. Large and pronounced differences in $\delta_{C\text{-}11}$ and $\delta_{C\text{-}8}$ shifts for phenolate and phenolic forms exclude their simultaneous formation in solution.

Comparison of antibacterial activity tests against Gram-(+) strains of **1** and derivatives **2–9** (Tables 1 and 5S†) showed extremely high activities of **1** and **9**. Antibacterial activity of compounds **2–8** is comparable to or even higher than that of the well known antibacterial agent ciprofloxacin (CIP – Table 1).

The question of why compounds **2–8** reveal lower activity than **1** and **9** arises. In attempt to answer this question the analysis of possible interactions at the binding site to RNAP (Fig. 3) was carried out. In the crystal structure reported by Campbell *et al.*[3a] the docking of **1** (yellow) at the binding site to RNAP is mainly achieved *via* hydrogen bonds (yellow colour) between the *ansa*-bridge groups and the amino acid residues as well as *via* some hydrophobic interactions. As we have shown, in the presence of H_2O, **1** exists as a zwitterion with a proton attached to N(40) atom and not in the uncharged phenolic form as suggested earlier.[3] Docking of the phenolate form of **1** into the crystal structure of RNAP[3a] (grey – Fig. 3a) and a simple rotation around the C(38)–N(38) bond of the protonated piperazine group revealed the possibility of formation of the earlier overlooked relatively strong hydrogen bond (length 2.6 Å, angle 170°) between $N(40)^{+}$–H and the carboxylate group of E_{445}. This intermolecular hydrogen bond with the carboxylate of E_{445} should contribute to the extremely high antibacterial activity of **2** and **9**, if one considers the lower activity of compounds **2–8**, for whose structures no similar interaction can be realised at the RNAP binding site (Fig. 3b). It should be emphasized that when **1** and **2** were docked as zwitterions, in the form observed in their crystal structures (Fig. 3a and b), the other important interactions between the *ansa*-bridge groups and the amino acid residues of RNAP, as reported by Campbell *et al.*,[3a] are also possible.

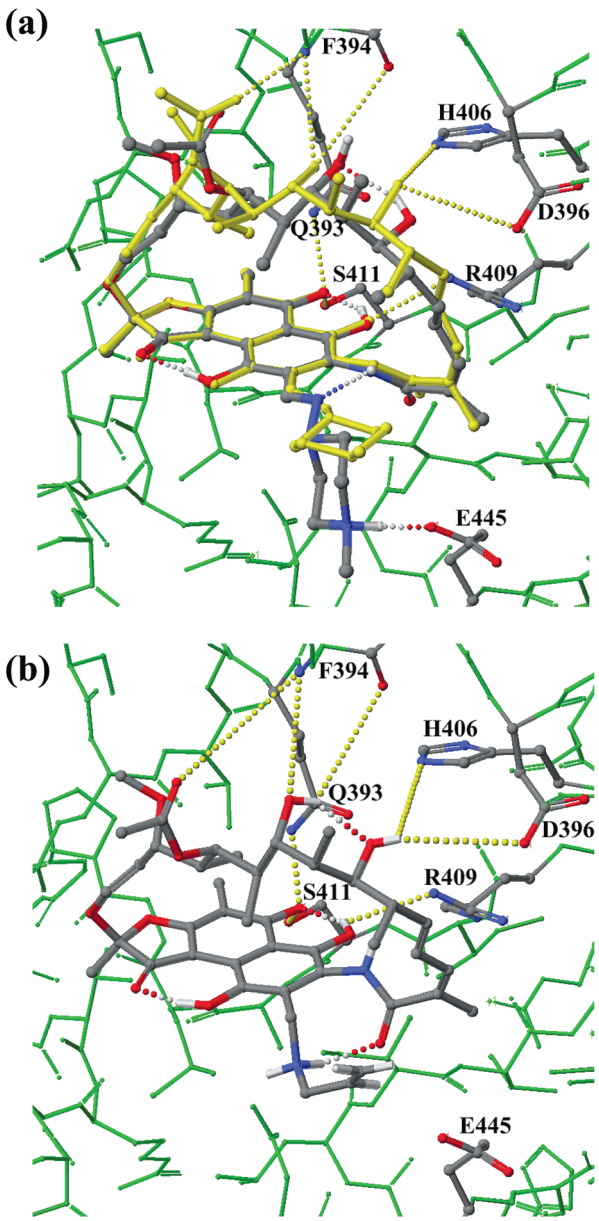

Fig. 3 Binding site to RNAP (green): (a) superposition of **1** phenolic form (yellow), docked according to Campbell *et al.*,[3a] with **1** zwitterionic form (grey), docked *via* and additional strong interaction with E_{445}, (b) docked X-ray structure of **2**. Other possible ligand–protein interactions are marked by yellow.

Thus, as we have demonstrated, the presence of phenolate form together with the localisation of the transferred proton at N (40) atom of piperazine moiety is crucial for extremely high biological activity of **1** and **9** in comparison to that of the derivatives **2–8**.

Acknowledgements

K.P. wishes to thank the Foundation for Polish Science and Adam Mickiewicz University Foundation for a fellowship. M.G.

and B.W. acknowledge support from the Polish Ministry of Science and Higher Education (grant No. N N204 212940).

Notes and references

1 E. Ngaimisi, S. Mugusi, O. Minzi, P. Sasi, K.-D. Riedel, A. Suda, N. Ueda, M. Janabi, F. Mugusi, W. E. Haefeli, L. Bertilsson, J. Burhenne and E. Aklillu, *Clin. Pharmacol. Ther.*, 2011, **90**, 406–413.
2 H. G. Floss and T.-W. Yu, *Chem. Rev.*, 2005, **105**, 621–632.
3 (*a*) E. A. Campbell, N. Korzheva, A. Mustaev, K. Murakami, S. Nair, A. Goldfarb and S. A. Darst, *Cell*, 2001, **104**, 901–912; (*b*) E. A. Campbell, O. Pavlova, N. Zenkin, F. Leon, H. Irschik, R. Jansen, K. Severinov and S. A. Darst, *EMBO J.*, 2005, **24**, 674–682; (*c*) I. Artsimovitch, M. N. Vassylyeva, D. Svetlov, V. Svetlov, A. Perederina, N. Igarashi, N. Matsugaki, S. Wakatsuki, T. H. Tahirov and D. G. Vassylyev, *Cell*, 2005, **122**, 351–363.
4 A. Bacchi, G. Pelizzi, M. Nebuloni and P. Ferrari, *J. Med. Chem.*, 1998, **41**, 2319–2332.
5 P. Ferrari and G. G. Gallo, *Farmaco*, 1975, **30**, 676–696.
6 G. Tsukamoto, M. Taguchi and N. Aikawa, *Chem. Pharm. Bull.*, 1980, **28**, 2309–2317.
7 K. Bujnowski, L. Synoradzki, E. Dinjus, T. Zevaco, E. Augustynowicz-Kopec and Z. Zwolska, *Tetrahedron*, 2003, **59**, 1885–1893.
8 M. M. de Villiers, M. R. Caira, J. Li, S. J. Strydom, S. A. Bourne and W. Liebenberg, *Mol. Pharmaceutics*, 2011, **8**, 877–888.
9 M. Gadret, M. Goursolle, J. M. Leger and J. C. Colleter, *Acta Crystallogr., Sect. B: Struct. Crystallogr. Cryst. Chem.*, 1975, **31**, 1454–1462.

